An on-line continuous updating Gaussian mixture model for damage monitoring under time-varying structural boundary condition

Lei Qiu, Shenfang Yuan, Qiao Bao, Tianxiang Huang

AN ON-LINE CONTINUOUS UPDATING GAUSSIAN MIXTURE MODEL FOR DAMAGE MONITORING UNDER TIME-VARYING STRUCTURAL BOUNDARY CONDITION

Lei Qiu[1], Shenfang Yuan[1*], Qiao Bao[1], Tianxiang Huang[1]

[1] *The State Key Lab of Mechanics and Control of Mechanical Structures, Nanjing University of Aeronautics and Astronautics, 29 Yudao Street, Nanjing 210016, People's Republic of China.*
ysf@nuaa.edu.cn

ABSTRACT

Damage monitoring under time-varying structural boundary condition is one of the most difficult tasks in piezoelectric transducers (PZTs) and Lamb wave based SHM methods for engineering applications. Because the structural boundary changes such as variations in the tightness of bolts between structures can lead to false monitoring result even the structure is in health state. This paper proposes a Lamb wave based on-line continuous updating Gaussian Mixture Model (GMM) to study the problem. Based on the baseline GMM constructed by features of Lamb wave signals in structural health state, an on-line continuous updating GMM is studied to learn the dynamic changes of Lamb wave monitoring signals without any prior knowledge of damage patterns. The Kullback–Leibler (KL) divergence is used as a degradation index to estimate the structural damage by measuring the difference between the baseline GMM and the on-line GMM. The proposed method is validated on an aircraft steel beam. The validation results show that the method is effective for bolt hole crack growth monitoring under the time-varying changes in the tightness degree of the bolts.

KEYWORDS : *structural health monitoring, Lamb wave, Gaussian mixture model , time-varying structural boundary condition*

INTRODUCTION

Among the existing SHM methods for aerospace structures, much attention has been paid to piezoelectric transducers (PZTs) and Lamb wave based SHM method because this method is regional monitoring, sensitive to inner small damage of structures, and can both be applied for damage and impact monitoring [1]. Most of the current PZTs and Lamb wave based SHM methods depend on the Lamb wave baseline signal acquired in the health state of the structure. And then, Lamb wave monitoring signals can be acquired on-line when the structure is in service. The state of the structure can be determined by using some SHM algorithms [2-7] to measure the difference between the Lamb wave baseline signal and the Lamb wave monitoring signals. Such a process can be implemented well in laboratory for the steady structural boundary condition.

The variations of Lamb wave properties can be a result of time-varying condition, such as environmental condition, operational condition and structural boundary condition [8-9]. Environmental condition includes temperature, humidity and noises, etc, while operational conditions includes random dynamic load, operation speed, vibration, etc. Structural boundary condition is often referred to structural surroundings or connection condition, such as variations of bolts tightness degree, thermal expansion and changes of connections between structures. The effect of structural boundary condition variation can be considered as two aspects. The first aspect is that the boundary reflections in Lamb wave signals are changed. This effect can be restrained by direct wave extraction. But for complex aircraft structures, the boundary reflections and the direct wave are often mixed together and hard to be separated. The second aspect is that the structural dynamic

response is changed. As a type of ultrasonic wave propagating on the structure, the dynamic response of Lamb wave is changed correspondly.

The problem of damage monitoring under time-varying structural boundary condition has become one of the obstacles for deploying a PZTs and Lamb wave based SHM system to real in-service aircraft structure. Hence, many researchers in SHM field have studied the problem preliminarily in recent years. The proposed methods can be divided into the following two categories.

1) Many reference free damage monitoring methods are proposed [10-12]. They want to fulfill damage estimation directly by using Lamb wave monitoring signals which are independent on Lamb wave baseline signals. The basic idea of these methods is that damage induced signals can be extracted through Lamb wave monitoring signals by using special sensors placement, advanced signal processing methods and Lamb wave modes modulation mechanisms. But the direct wave, boundary reflections and multi-modes of Lamb wave signals are often mixed together closely on complex structures and almost impossible to be distinguished.

2) Many researchers conduct studies on data normalization models combining with regression analysis, novelty detection and artificial neural network, etc [13-15]. When a set of Lamb wave baseline signals in health state of a structure are acquired over a wide range of time-varying structural boundary condition, baseline model can be constructed by using their features. Once the features of Lamb wave monitoring signals are out of baseline model, the abnormal condition of the structure can be detected. These methods are feasible but need further studies.

Gaussian Mixture Model (GMM) [15] which is frequently used in the field of computer science for pattern recognition and classification, is a typical probability statistical model based on unsupervised learning to organize itself according to the nature of the input data with complicated probability distributions. The random effects produced by time-varying structural boundary condition are regarded as mixture probability distributions. Once the GMM shows a cumulative progressive trend, the damage can be identified. Banerjee and Qing[17] first attempt implementing the GMM to address the problem of progressive crack monitoring under continuous cyclic loading condition. In their research, the Lamb wave monitoring signals acquired in the whole process of crack growth are divided into many data subsets. The GMM is constructed on each data subset and Mahalanobis distance which is considered to be a damage index is used to measure the difference between the GMMs. It represents the process of crack growth well in the validation experiments.

This paper attempts another realization of GMM based damage monitoring method. In which, the baseline GMM is constructed on features of Lamb wave signals in health state of a structure, an on-line continuous updating GMM is used to learn the dynamic changes of Lamb wave monitoring signals. The Kullback–Leibler (KL) divergence is used as a degradation index to estimate the structural damage by measuring differences between the baseline GMM and the on-line GMM. The features of Lamb wave signals are obtained by using damage index calculation and Principle Component Analysis (PCA).

1 DAMAGE INDEX CALCULATION

In this paper, four kinds of damage index are adopted and shown as following equations from (1) to (4), where $b(t)$ and $m(t)$ represent the Lamb wave baseline signal and the Lamb wave monitoring signal respectively, where t_0 and t_1 are the start and stop time corresponding to the selected signal time window.

1) Damage index 1 (DI_1) is the time domain cross-correlation shown in Equation (1).

$$DI_1 = 1 - \frac{\int_{t_0}^{t_1} \left(b(t) - \mu_{b(t)}\right)\left(m(t) - \mu_{m(t)}\right) dt}{\sigma_{b(t)} \sigma_{m(t)}} \tag{1}$$

Where, $\mu_{b(t)}$ and $\mu_{m(t)}$ are the mean value of the signals, $\sigma_{b(t)}$ and $\sigma_{m(t)}$ are the variance of the signals.

2) Damage index 2 (DI_2) is the time domain difference shown in Equation (2) [18].

$$DI_2 = \int_{t=t_0}^{t_1} \tilde{d}^2(t) dt \tag{2}$$

Where, $\tilde{D}(t) = \dfrac{m(t)}{\sqrt{\int_{t=t_0}^{t_1} m^2(t) dt}}$, $\alpha = \dfrac{\int_{t=t_0}^{t_1} \tilde{D}(t)b(t) dt}{\int_{t=t_0}^{t_1} b^2(t) dt}$, $\tilde{d}(t) = \tilde{D}(t) - \alpha b(t)$

3) Damage index 3 (DI_3) is called spectrum magnitude difference shown in Equation (3).

$$DI_3 = \sqrt{\dfrac{\int_{\omega_0}^{\omega_1} \left(|b(\omega)| - |m(\omega)|\right)^2 d\omega}{\int_{\omega_0}^{\omega_1} |b(\omega)|^2 d\omega}} \tag{3}$$

Where, $b(\omega) = \int_{t_0}^{t_1} b(t)e^{-j\omega t} dt$ and $m(\omega) = \int_{t_0}^{t_1} m(t)e^{-j\omega t} dt$, where ω_0 and ω_1 are the start and stop frequency corresponding to the selected signal spectrum window.

4) Damage index 4 (DI_4) is called frequency domain cross-correlation shown in Equation (4).

$$DI_4 = 1 - \dfrac{\int_{\omega_0}^{\omega_1} b(\omega)m(\omega) d\omega}{\sqrt{\int_{\omega_0}^{\omega_1} b^2(\omega) d\omega \int_{\omega_0}^{\omega_1} m^2(\omega) d\omega}} \tag{4}$$

Till now, many damage indexes are proposed to quantification the difference between the Lamb wave baseline signal and the Lamb wave monitoring signal [19]. The damage indexes adopted in this paper are not limited to them only.

These damage indexes still have noises, and the dimension of the feature vector constructed by them maybe big to be used as the GMM inputs, especially when more damage indexes are used. Due to the dimension reduction and global information preservation capability of PCA, it is used on the damage indexes to extract the feature vector composed by principle components.

2   GMM AND ON-LINE CONTINUOUS UPDATING

The whole framework of the on-line continuous updating GMM based damage monitoring method under time-varying structural boundary condition is shown in Figure 1, which includes two parts, namely the baseline GMM and on-line GMM.
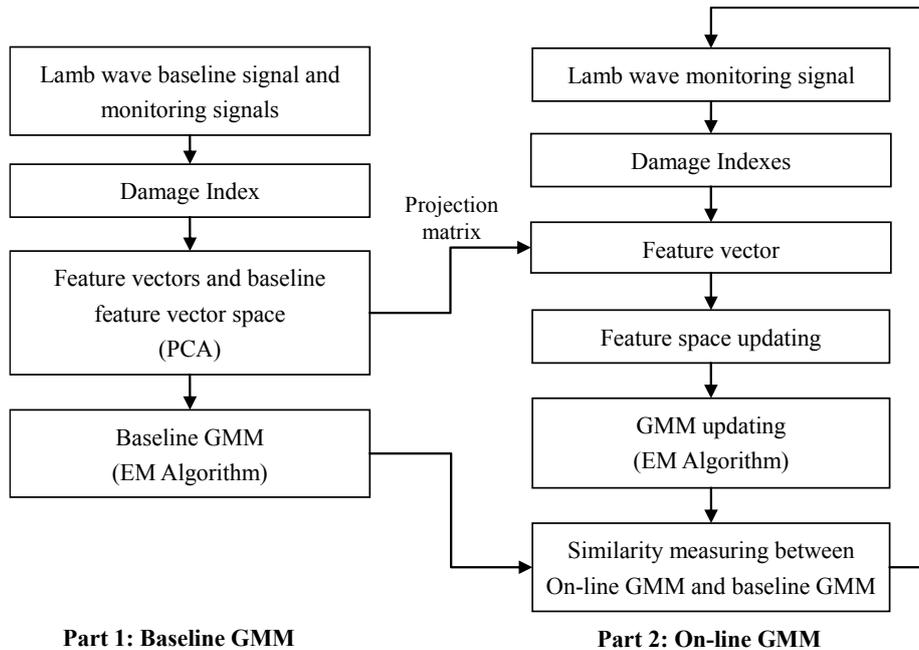

Figure 1: The framework of the on-line continuous updating GMM based damage monitoring method

In the baseline GMM part, Lamb wave signals are acquired under time-varying structural boundary condition when the structure is in health state. Considering that the first Lamb wave signal is the baseline signal and the other Lamb wave signals are the monitoring signals, four kinds of damage index which are discussed in section 1 can be obtained by comparing the monitoring signals with the baseline signal. The feature vectors are extracted through fusion the four damage indexes by PCA to span a feature space of the healthy structure, and then the baseline GMM is constructed on the feature space by using Expectation Maximization (EM) algorithm [15]. The principle projection matrix obtained by PCA is kept for calculating the feature vector in the on-line GMM part.

Without loss generation, $\mathbf{FV}^b$ is denoted as the baseline feature space. $F^b=[F_1, F_2,...., F_d]$ is set to be a d-dimensional random variable and represents a feature vector of $\mathbf{FV}^b$. The numbers of feature vectors in $\mathbf{FV}^b$ is k. $f^b=[f_1,f_2,..., f_d]$ is a particular outcome of F^b. In this paper, $d=2$. Supposing that F^b follows a finite mixture distribution when its probability density function $\mathbf{\Phi}^b(f)$ can be written as a finite weighted sum of Gaussian densities $\Phi^b_i(f)$ with mean μ^b_i and covariance matrix Σ^b_i, the baseline GMM with C Gaussian components can be written as follows.

$$\mathbf{\Phi}^b\left(f^b \middle| \Theta^b\right) = \sum_{i=1}^{C} w^b_i \Phi^b_i\left(f^b \middle| \Theta^b_i\right) \qquad (5)$$

Where w^b_i is the mixture weight of i-th Gaussian component and Θ^b_i is consisting of unknown Gaussian distribution parameters μ^b_i and Σ^b_i. Θ^b is the Gaussian distribution parameters μ^b and Σ^b of the baseline GMM. In this paper, the numbers of Gaussian components is set to be $C=3$.

The value of Θ^b_i is calculated by using EM algorithm which is consisted of Expectation calculation step (E-step) and Maximum likelihood estimation step (M-step). The initial value of Θ^b_i and w^b_i are set first. And then, in E-step, the maximum likelihood of each Gaussian component is calculated based on $\mathbf{FV}^b$ and the K-means algorithm. In M-step, the maximum likelihood of each Gaussian component is updated. After multiple iterations between E-step and M-step, the optimization value of Θ^b_i and w^b_i are obtained. Finally, the parameters μ^b and Σ^b of Θ^b can be represented as Equation (6).

$$\mu^b = \sum_{i=1}^{C} w^b_i \cdot \mu^b_i \;, \quad \Sigma^b = \sum_{i=1}^{C} w^b_i \cdot \Sigma^b_i \qquad (6)$$

In the on-line GMM part, the Lamb wave monitoring signal is acquired one by one. When an new Lamb wave monitoring signal is acquired, the corresponding feature vector is obtained. And then the feature space is updated based on the newly obtained feature vector and an new GMM is generated by using the EM algorithm. Finally, the baseline GMM will be used to compare with the on-line GMM to obtain the KL divergence.

The GMM is continuous updating by using the following steps, in which, n ($n \geqslant 1$) denotes the monitoring times in this part.

Step (1), A new feature vector $f(n)$ is generated according to the current acquired Lamb wave monitoring signal based on the method mentioned in section 1.

Step (2), Feature space updating: The old feature space $\mathbf{FV}(n\text{-}1)$ should be updated to generate new feature space $\mathbf{FV}(n)$. Particularly, $\mathbf{FV}(0)$ is the baseline feature space $\mathbf{FV}^b$. The feature space updating rule is called moving update which adds $f(n)$ into $\mathbf{FV}(n\text{-}1)$ to be the last (newest) feature vector and remove the first (oldest) feature vector of $\mathbf{FV}(n\text{-}1)$. Hence, the numbers of feature vectors in feature space $\mathbf{FV}(n)$ is still k.

Step (3), An new GMM denoted as $\mathbf{\Phi}^n$ and shown in Equation (7) is constructed on the feature space $\mathbf{FV}(n)$ by using EM algorithm.

$$\mathbf{\Phi}^n\left(f^n \middle| \Theta^n\right) = \sum_{i=1}^{C} w^n_i \Phi^n_i\left(f^n \middle| \Theta^n_i\right) \qquad (7)$$

Where Θ^n is the Gaussian distribution parameters μ^n and Σ^n, and w^n_i is the mixture weight of i-th Gaussian component of the current on-line GMM $\mathbf{\Phi}^n$.

Step (4), the degradation index calculation: The degradation index denoted as $D_{KL}(n)$ is calculated by measuring the difference between the baseline GMM and the on-line GMM combining with the KL-divergence. And then, go back to step (1) to continuously update the on-line GMM again when an new Lamb wave monitoring signal is acquired and set $n=n+1$.

The similarity between the baseline GMM and the on-line GMM can be used to estimate the degradation state of the structure caused by damage. There are many methods which can be used to measure the similarity or distance between two probability distributions. The KL divergence, which is usually used to measure the difference between two probability distributions in information theory, is adopted in this paper and is represented as Equation (8).

$$D_{KL}\left(\Phi^b, \Phi^n\right) = \frac{1}{2}\left(\text{tr}\left(\left(\Sigma^n\right)^{-1}\left(\Sigma^b\right)\right) + \left(\mu^n - \mu^b\right)^T \left(\Sigma^n\right)^{-1}\left(\mu^n - \mu^b\right) - C - \ln\left(\frac{\det \Sigma^n}{\det \Sigma^b}\right)\right) \quad (8)$$

There should be noted that it is not to estimate the damage size from the degradation index. It is only used to understand the change trend of the difference between the on-line GMM and the baseline GMM companying with the growth of the damage.

3   VALIDATION EXPERIMENT OF THE METHOD

The validation experiment is performed on an aircraft steel main beam shown in Figure 2. There are many beam bolts, which are used to connect the beam with wing skin, distribute on the beam edge zone 1 in equal interval distance. The bolts numbered 1 to 5 are considered in the experiment.
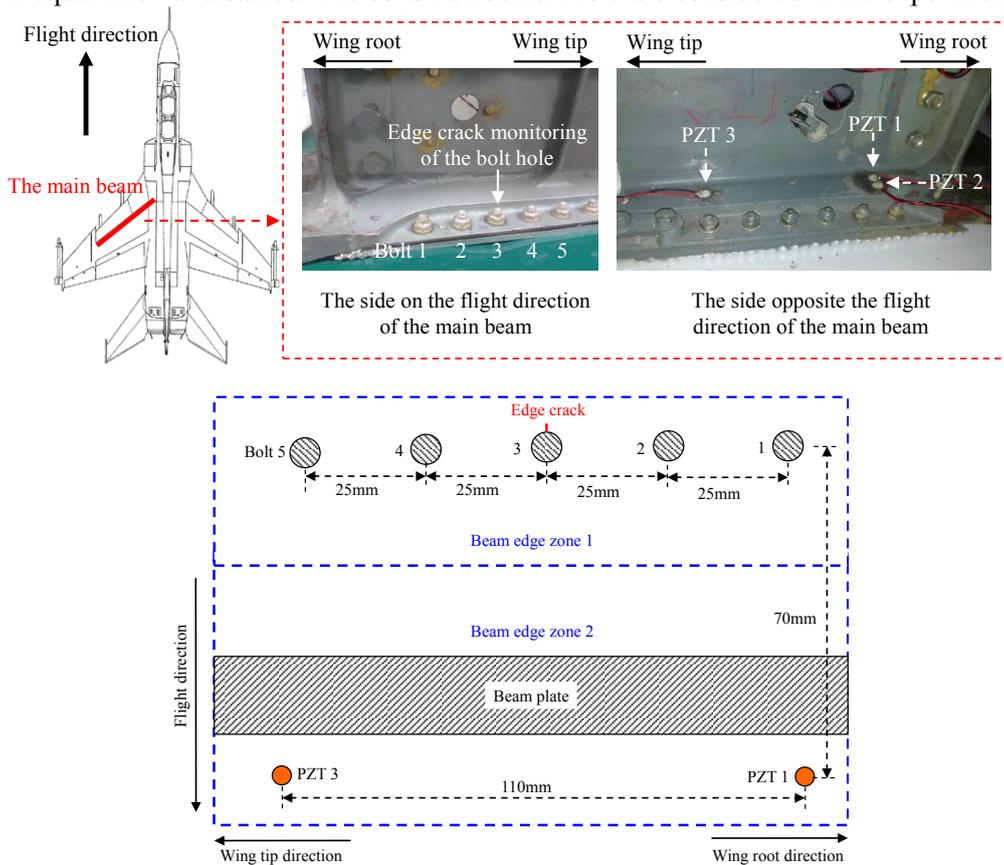

Figure 2: The aircraft main beam and PZTs placement

The inner space of the aircraft structure in the side on the flight direction of the main beam is very small. No sensors can be placed in it and the NDT is hard to be applied. But the edge crack of the bolt hole is the main damage form of the aircraft structure. The sensors can only be placed on

the opposite side of the flight direction of the main beam. Hence, three PZTs are placed on the beam edge zone 2, but PZT 1 and PZT 3, which are set to be actuator and sensor respectively, are only used in the experiment. The thickness of zone 1 and zone 2 are 20.8mm and 9.70 mm, respectively.

The time-varying structural boundary condition is introduced through loosing the bolts in different degree manually. The edge crack of bolt hole 3 is produced by wire-electrode cutting. The experiment is used to validate the crack growth monitoring ability of the method under the time-varying changes in the tightness degree of the bolts.

The integrated multi-channel scanning system developed by the authors [20] is adopted to be the Lamb wave excitation and acquisition system in this experiment. The central frequency of five-peak wave excitation signal is 200kHz and the sampling rate is 10M samples/s.

In the baseline GMM part, the Lamb wave signals are acquired in the following steps. Step (1): Acquire Lamb wave baseline signal when all the bolts are tight. Step (2): Loose one bolt and acquire a Lamb wave monitoring signal, and then, fasten the bolt and acquire a Lamb wave monitoring signal. Repeat this process on each bolt respectively. Step (3): Repeat step (2) two times. There totally 31 Lamb wave monitoring signals are acquired.

In the on-line GMM part, the Lamb wave monitoring signals are acquired in the following steps. Step (1) : Repeat the step (2) in the baseline GMM part two times. Step (2) : Remove bolt 3 and produce a crack of 1mm length at the hole edge. And then, fasten bolt 3. Step (3) : Repeat the step (1). Step (4) : Remove bolt 3 and extend the crack length to 2mm. And then, fasten bolt 3. Step (5) : Repeat the step (1). Step (6) : Remove bolt 3 and extend the crack length to 3mm. And then, fasten bolt 3. Step (7) : Repeat the step (1). There totally 80 Lamb wave monitoring signals are acquired. They are used to update the on-line GMM continuously one by one.

Figure 3 (a) gives out a typical signal comparison between the Lamb wave monitoring signals and the Lamb wave baseline signal. It first indicates that the boundary reflections, crack reflections and A_0 mode are mixed together. Second, the difference between the baseline signal and the monitoring signal caused by crack is mixed into the difference caused by bolt loosening. In traditional damage index based methods, a damage threshold is often predefined. When the value of damage index exceeds the threshold, the damage occurrence can be determined. These methods perform well in laboratory static structural boundary condition, but the crack growth are hard to be recognized directly because of the damage indexes random variations which are mainly caused by the time-varying structural boundary condition shown in Figure 3(b).

The feature vectors corresponding to the first 30 Lamb wave monitoring signals obtained by PCA are used to build a two-dimensional feature space and the baseline GMM constructed on the feature space is shown in Figure 4(a). The baseline GMM contains three Gaussian components and the feature space is covered by it.
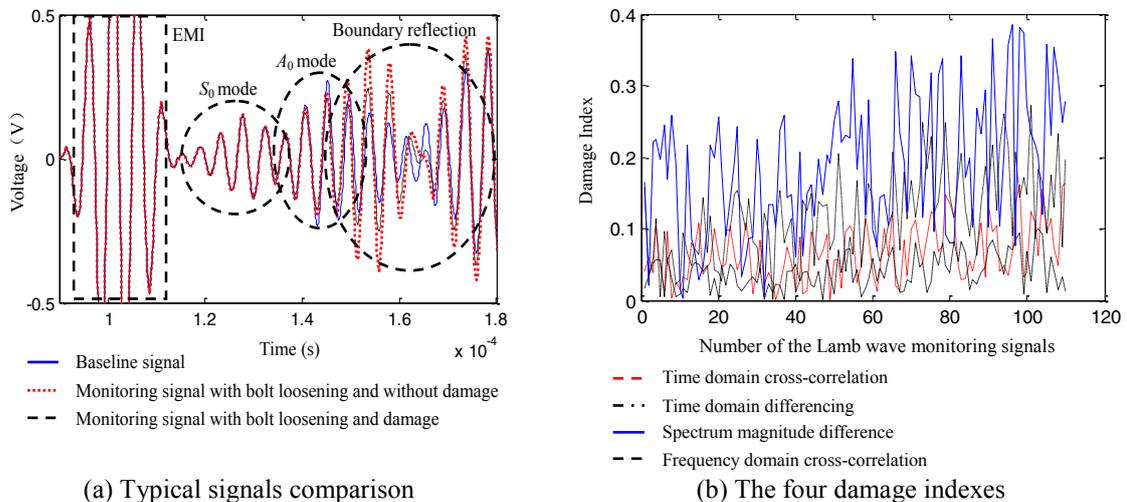
(a) Typical signals comparison (b) The four damage indexes

Figure 3: Typical signals comparison and the damage indexes of Lamb wave monitoring signals

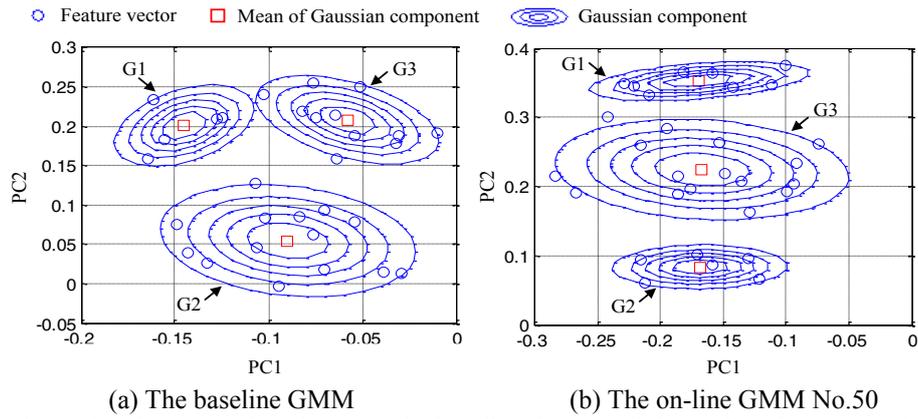(a) The baseline GMM   (b) The on-line GMM No.50

Figure 4: The comparison between the baseline GMM and the on-line GMM No.50
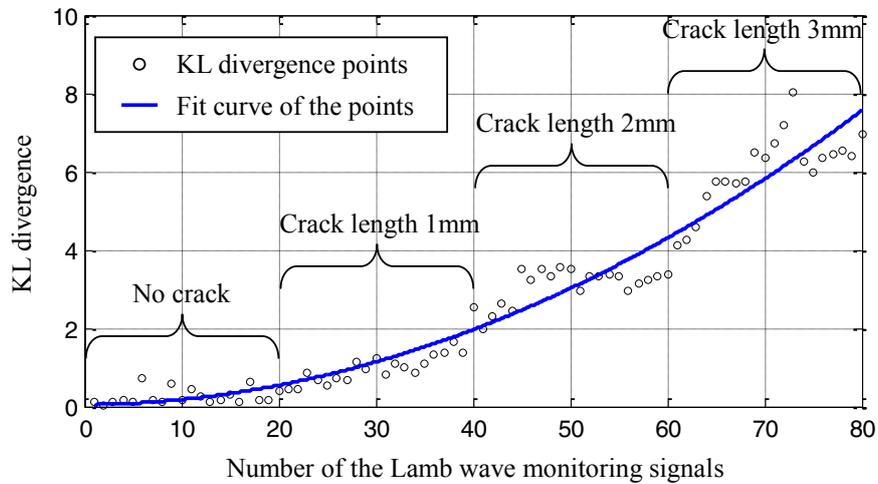

Figure 5: The results of KL divergence degradation index

The obtained on-line GMM No.50 when the crack length is 2mm, is shown in Figure 4(b), which indicates that the three Gaussian components have seriously drift from the original position because of the damage. The final results of the KL divergence are shown in Figure 5 which represents the crack growth well under the time-varying structural boundary condition. When the structure is in health state, the random variations of the structural boundary condition make little influence on the KL divergence. But when a progressive damage is generated and extended, the KL divergence shows a cumulative increasing trend.

CONCLUSION

An on-line continuous updating GMM is proposed to fulfill the damage monitoring under time-varying structural boundary condition. The feature vectors which are used to construct the GMM are obtained by PCA based on the four damage indexes. The GMM is updated on-line by feature vectors of the Lamb wave monitoring signals one by one. The KL-divergence is used as a degradation index to measure the difference between the on-line GMM and the baseline GMM to present the damage monitoring results. The results of the validation experiment performed on an aircraft steel beam show that the on-line continuous GMM can identify the cumulative increasing trend caused by the crack growth.

REFERENCES

[1] C. Boller, F. K. Chang, Y. Fujino. *Encyclopedia of Structural Health Monitoring*. John Wiley and Sons, Ltd. 2009.

[2] L.Wang, F. G. Yuan. Active Damage Localization Technique Based on Energy Propagation of Lamb Waves. *Smart Structures and Systems*, 3: 201–217, September 2007.

[3] J. Staszewski, S. Mahzan, R. Traynor. Health Monitoring of Aerospace Composite Structures-Active and Passive Approach. *Composites Science and Technology*, 69:1678–1685, September 2009.

[4] A. Shelke, T. Kundu, U. Amjad, K. Hahn, and W. Grill. Mode-Selective Excitation and Detection of Ultrasonic Guided Waves for Delamination Detection in Laminated Aluminum Plates. *IEEE Transactions on Ultrasonics, Ferroelectrics and Frequency Control,* 58: 567–577, March 2011.

[5] P. Malinowskia, T. Wandowskia, W. Ostachowicz. Damage Detection Potential of A Triangular Piezoelectric Configuration. *Mechanical Systems and Signal Processing*, 25: 2722–2732, October 2011.

[6] L. Y. Yu, V. Giurgiutiu, J. J. Wang, Y. J. Shin. Corrosion Detection with Piezoelectric Wafer Active Sensors Using Pitch-catch Waves and Cross-Time-Frequency Analysis. *Structural Health Monitoring*, 11: 83–93, January 2012.

[7] L. Qiu, M. L. Liu, X. L. Qing, and S. F. Yuan. A Quantitative Multi-Damage Monitoring Method for Large-Scale Complex Composite. *Structural Health Monitoring,* 12:183–196, May 2013.

[8] H. Sohn. Effects of Environmental and Operational Variability on Structural Health Monitoring. *Philosophical Transactions of the Royal Society A*, 365:539–560, February 2007.

[9] I. Lopez, and N. Sarigul-Klijn. A Review of Uncertainty in Flight Vehicle Structural Damage Monitoring, Diagnosis and Control: Challenges and Opportunities. *Progress in Aerospace Sciences*, 46: 247–273, October 2010.

[10] Q. Wang, S. F. Yuan. Baseline-free Imaging Method based on New PZT Sensor Arrangements. *Journal of Intelligent Material Systems and Structures*, 20:1663-1673, May 2009.

[11] H. Sohn. Reference-Free Crack Detection under Varying Temperature. *KSCE Journal of Civil Engineering*, 15:1395–1404, February 2011.

[12] H. J. Lim, H. Sohn, C. M. Yeum, and J. M. Kim. Reference-free damage detection, localization,and quantification in composites. *The Journal of the Acoustical Society of America*, 133: 3838–3845, June 2013.

[13] K. K. Nair, A. S. Kiremidjian, and K. H. Law. Time Series-Based Damage Detection and Localization Algorithm with Application to the Asce Benchmark Structure. *Journal of Sound and Vibration*, 291: 349–368, March 2006.

[14] K. Worden and G. Manson. The Application of Machine Learning to Structural Health Monitoring. *Philosophical Transactions of the Royal Society A: Mathematical, Physical and Engineering Sciences*, 365: 515–37, February 2007.

[15] C. K. Oh, and H. Sohn. Damage Diagnosis under Environmental and Operational Variations Using Unsupervised Support Vector Machine. *Journal of Sound and Vibration*, 325: 224–239, August 2009.

[16] J. A. Bilmes. A Gentle Tutorial of the Em Algorithm and Its Application to Parameter Estimation for Gaussian Mixture and Hidden Markov Models. *International Computer Science Institute*, TR-97-021, April 1998.

[17] S. Banerjee, X. L. Qing, S. Beard, F.K. Chang. Prediction of Progressive Damage State at the Hot Spots using Statistical Estimation. *Journal of Intelligent Material Systems and Structures*, 21: 595-605, February 2010.

[18] J. E. Michaels, T. E. Michaels. Detection of Structural Damage from the Local Temporal Coherence of Diffuse Ultrasonic Signals. *IEEE Transactions on Ultrasonics, Ferroelectrics, and Frequency Control*, 52:1769-1782, October 2005.

[19] Z. Q. Su, L. Ye. Identification of Damage Using Lamb Waves: From Fundamentals to Applications. Lecture Notes in Applied and Computational Mechanics, 2009.

[20] L. Qiu, S. F. Yuan. On Development of a Multi-Channel PZT Array Scanning System and Its Evaluating Application on UAV Wing Box. *Sensors and Actuators A, Physical*, 151: 220-230, April 2009.